Geological Society of America
Special Paper 229
1988

The 1929 "Grand Banks" earthquake, slump, and turbidity current

David J. W. Piper, *Atlantic Geoscience Centre, Geological Survey of Canada, Bedford Institute of Oceanography, P.O. Box 1006, Dartmouth, Nova Scotia B2Y 4A2, Canada*
Alexander N. Shor, *Lamont-Doherty Geological Observatory of Columbia University, Palisades, New York 10964*
John E. Hughes Clarke, *Department of Oceanography, Dalhousie University, Halifax, Nova Scotia B3H 4J1, Canada*

ABSTRACT

The epicenter of the 1929 "Grand Banks" earthquake (M_S = 7.2) was on the continental slope above the Laurentian Fan. The zone in which cables broke instantaneously due to the earthquake is characterized by surface slumping up to 100 km from the epicenter as shown by sidescan sonographs and seismic reflection profiles. The uppermost continental slope, however, is almost undisturbed and is underlain by till deposited from grounded ice.

The Eastern Valley of the Laurentian Fan contains surficial gravels molded into large sediment waves, believed to have formed during the passage of the 1929 turbidity current. Sand sheets and ribbons overlie gravel waves in the lower reaches of Eastern Valley. Cable-break times indicate a maximum flow velocity of 67 km/hr (19 m/s). The occurrence of erosional lineations and gravel on valley walls and low intravalley ridges suggest that the turbidity current was several hundred meters thick. The current deposited at least 175 km^3 of sediment, primarily in a vast lobe on the northern Sohm Abyssal Plain where a bed more than 1 m thick contains material ranging in size from gravel to coarse silt.

There is no apparent source for so much coarse sediment on the slumped areas of the muddy continental slope. We therefore infer that there was a large volume of sand and gravel available in the upper fan valley deposits before the earthquake. This coarse sediment was discharged from sub-glacial meltwater streams when the major ice outlet through the Laurentian Channel was grounded on the upper slope during middle Wisconsinan time. This sediment liquefied during the 1929 event, and the resulting flow was augmented by slumping of proglacial silts and gas-charged Holocene mud on the slope. Although earthquakes of this magnitude probably have a recurrence interval of a few hundred years on the eastern Canadian margin, we know of no other deposits of the size of the 1929 turbidite off eastern Canada. For such convulsive events, both a large-magnitude earthquake and a sufficient accumulation of sediment are required.

GEOLOGIC SETTING

The epicenter of the "Grand Banks" earthquake of November 18, 1929, was located on the continental slope between St. Pierre Bank and the Laurentian Fan, at the extreme western margin of the Grand Banks of Newfoundland (Fig. 1). This part of the continental slope appears to be a typical passive margin developed during the late Triassic rifting of the central Atlantic Ocean (Haworth and Keen, 1979). It is more than 60 km from the northwest-to-southeast-trending transform margin along the Southwestern Grand Banks Slope that marks the northeastern extent of the Mesozoic central Atlantic Ocean. The epicenter lies south of a major, east-west, Late Paleozoic strike-slip fault zone on the outer continental shelf (Chedabucto Fault on the Scotian Shelf, Collector anomaly on the Grand Banks: Haworth and Keen, 1979). The Mesozoic–Tertiary continental margin sediment wedge beneath the continental slope near the 1929 epicenter is up to 8 km thick (Uchupi and Austin, 1979).

The surface morphology of the continental margin south

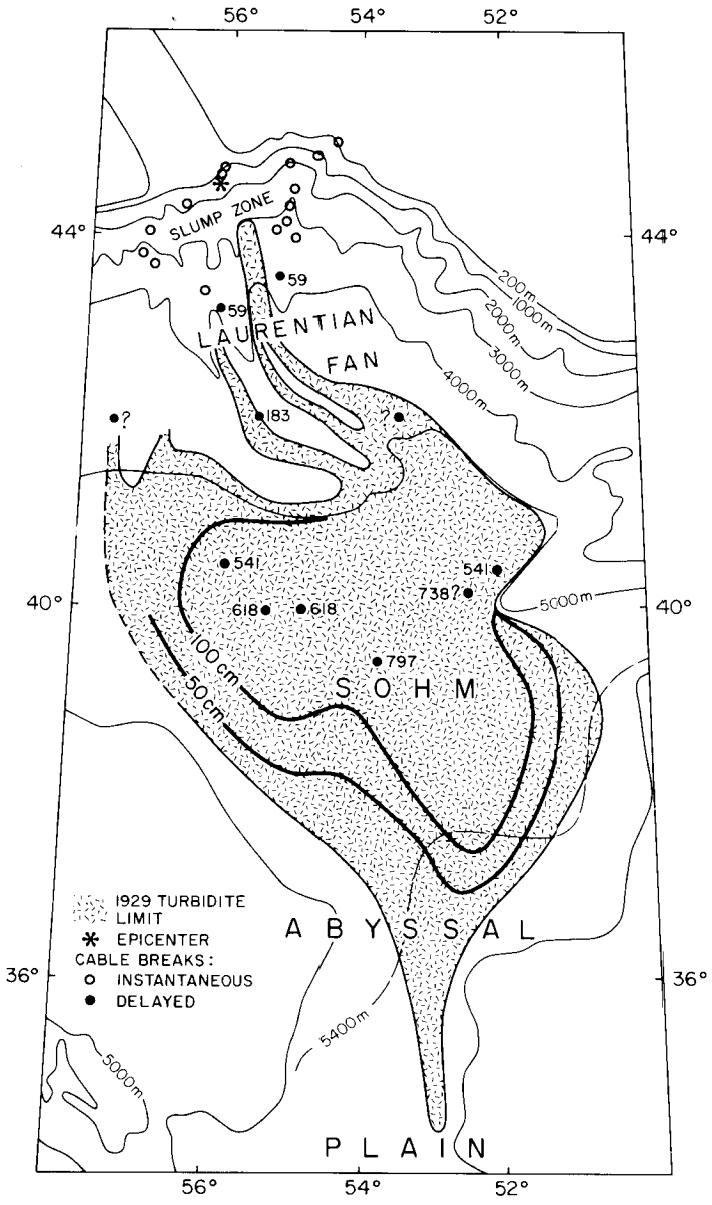

Figure 1. Map showing cable breaks and thickness of turbidite deposit resulting from the 1929 earthquake. Epicenter from Dewey and Gordon (1984). Location and time (minutes after main shock) of cable breaks from Doxsee (1948). Limit and isopachs of turbidite on the Sohm Abyssal Plain from Fruth (1965) and Piper and Aksu (1987).

and west of the Grand Banks is the result of late Tertiary and Quaternary geomorphic processes. The 400-m-deep U-shaped trough of the Laurentian Channel was glacially excavated in the Pleistocene along the locus of a late Tertiary fluvial system (King and MacLean, 1970). It was the major ice outlet for a large area bordering on the Gulf of St. Lawrence, and large quantities of glacial sediment passed through it to the continental slope above the Laurentian Fan (Stow, 1981). The continental slope seaward of the Laurentian Channel shows net late Quaternary erosion, following a phase of late Tertiary–early Quaternary progradation (Piper and Normark, 1982b). In contrast, the slope off St. Pierre Bank shows progradation throughout much of the Quaternary, broken only by minor erosional events (Meagher, 1984). High-resolution seismic profiles from the St. Pierre Slope show till tongues, indicating the presence of grounded ice, extending to water depths of 500 m (Piper and others, 1984b). Pebbly mudstones that outcrop in the upper fan valleys are probably of glaciomarine origin.

The Laurentian Fan is a major deep-water sediment accumulation seaward of the Laurentian Channel. Several tributary valleys on the continental slope lead to two main valleys (Eastern and Western) (Masson and others, 1985) that extend to water depths of about 5,000 m, where they debouch onto the Sohm Abyssal Plain (Fig. 2). Regional bathymetric and seismic data indicate that the valleys off the Grand Banks do not contribute significant amounts of sediment to the fan.

The upper Western Valley, which drains the slope south of the Laurentian Channel, and the Central Valley, which drains the region between the Eastern and Western Valleys, join near the 3,600-m isobath to form the main Western Valley (Fig. 2). Its floor is around 3 to 5 km wide, and the valley becomes sinuous below 4,000 m.

The Eastern Valley floor is typically 25 km wide, with a western levee that stands as much as 950 m above the valley floor. The tributary Grand Banks Valley (Fig. 2) drains the slope between St. Pierre Bank and Whale Bank, forming a major reentrant feature into the upper slope. The Eastern Valley splits into two branches below 4,300 m, the east and the south branches. The Eastern Valley has been the locus of much of the recent research into the effects of the 1929 event (Piper and others, 1985a; Hughes Clarke, 1986). In this chapter, the term "upper valley" refers to Eastern Valley above 2,000 m water depth, "middle valley" to 2,000 to 4,500 m, and "lower valley" to below 4,500 m.

South of 42°N, both the Eastern and Western valleys turn to the ESE (Normark and others, 1983). Beyond this region, which is termed the valley termination zone (Piper and others, 1984a), the valleys are reduced to shallow low depressions whose axis and trend are very poorly defined.

METHODS AND DATA

This paper reviews a large amount of mostly unpublished data collected between 1981 and 1985 in the area of the 1929 earthquake epicenter and turbidite, as well as drawing on earlier published work on the 1929 event and the regional studies of Stow (1981) and Piper and his co-workers (Piper and Normark, 1982b; Normark and others, 1983; Piper and others, 1984a). SeaMARC I mid-range sidescan data were collected around the epicenter of the 1929 earthquake (Piper and others, 1985a) and along much of the length of Eastern Valley (Hughes Clarke, 1986) on cruises in 1983 and 1984. About 20 new piston cores from the epicentral region and Eastern Valley were obtained on

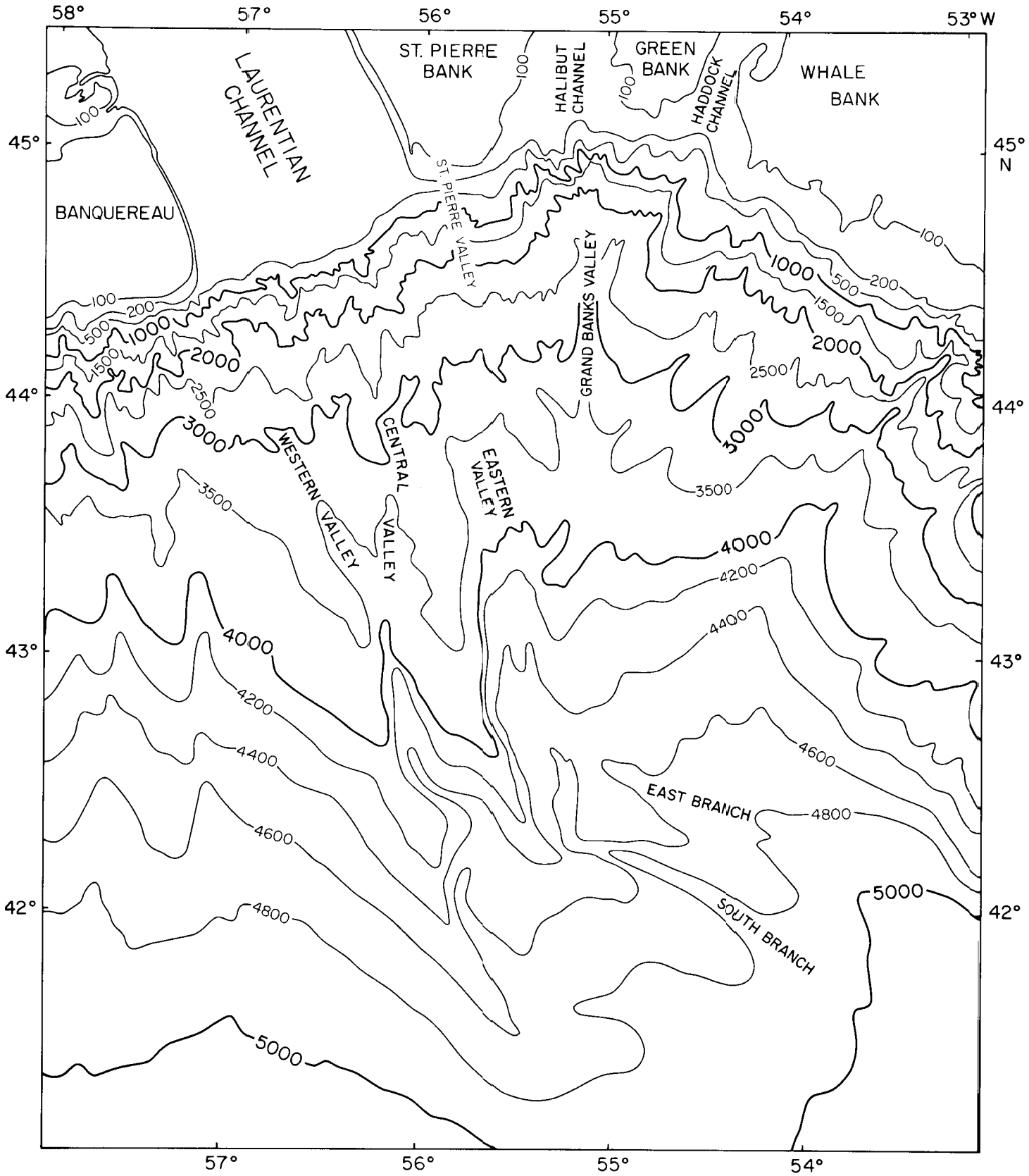

Figure 2. Bathymetry of Laurentian Fan north of 41°N. Compilation based on Canadian Hydrographic Survey charts 801 and 802, updated using C.H.S. chart Nk 21-B and echo-sounding data from Bedford Institute of Oceanography cruises 78-022 and 83-017. Contour intervals are 100 m, 200 m, then at 500 m to 4,000 m, and 200 m to 5,000 m.

three cruises between 1981 and 1985. A bottom camera system was used to obtain seabed photographs in 1985. Both cores and photographs allow detailed interpretation of acoustic facies identified in sidescan images. Four dives were made using the Pisces IV submersible in 1985 in the epicentral region and the uppermost part of Eastern Valley. Bathymetric, 3.5-kHz, and seismic profiles were obtained on most of these cruises.

THE 1929 EARTHQUAKE

Location and magnitude

The Grand Banks earthquake occurred at 2032 Z on November 18, 1929. There was a pronounced aftershock at about 2302 Z. The most recent relocation by Dewey and Gordon (1984) places the epicenter at 44°41.5′N 56°00.4′W, with $M_S = 7.2$.

Effects of the earthquake

The Grand Banks earthquake is known for the remarkable series of cable breaks on the ocean floor south of the epicenter (Doxsee, 1948). These breaks were used by Heezen and Ewing (1952) and Heezen and others (1954) to propose the occurrence of a large turbidity current. The earthquake was also responsible for 27 of the 28 recorded earthquake-related deaths in Canadian history. The summary of the earthquake effects presented here is based on Doxsee (1948). We have also used his numbering of cable breaks throughout this paper.

Severe seismic-shock effects on land were restricted to southeastern Cape Breton Island, where some chimneys fell and highways were blocked by small landslides. Four ships at sea within 250 km of the epicenter reported severe tremors (de Smitt, 1932).

The tsunami associated with the earthquake coincided with a storm high tide, accentuating its effect and making it difficult to accurately reconstruct the behavior of the tsunami itself. Most damage occurred in southwestern Placentia Bay, on the south coast of Newfoundland, particularly in places where the tsunami was funneled and concentrated by local relief. The tsunami was also detected in Halifax, Nova Scotia, and the islands of Bermuda and the Azores.

Twenty-eight breaks were reported in 12 different cables in the area around and to the south of the epicenter (Fig. 1). The time of five of these breaks is unknown, and 12 are recorded as instantaneous at the time of the earthquake. The remaining 11 cables broke at times up to 13 hr after the earthquake, approximately in sequence from north to south. The instantaneous breaks, within 100 km of the epicenter, were interpreted by Heezen and Ewing (1952) to result from sediment failure around the epicenter, whereas the sequential breaks resulted from a turbidity current. The distances between successive cable breaks imply current velocities of at least 67 km/hr on the upper fan, decreasing to 32 km/hr on the northern Sohm Abyssal Plain, 550 km south of the epicenter. (These estimates are reviewed in detail below.)

FAILURE ON THE CONTINENTAL SLOPE

The distribution and style of failure on the continental slope (Fig. 3) around the earthquake epicenter is known from SeaMARC I 5-km-swath side-scan sonar surveys (Piper and others, 1985a). High-resolution seismic reflection profiles, cores (Piper and others, 1984b), bottom photographs, and 27 hr of Pisces IV submersible observation have provided further ground truth.

The present morphology of the continental slope off the Laurentian Channel appears to be largely erosional relief in Pleistocene muds and pebbly mudstones (Fig. 4). The valleys of the Laurentian Fan are floored by gravel and sand, with a veneer of overlying mud. The uppermost part of the slope off St. Pierre Bank is underlain by glacial till, which interfingers downslope with proglacial silt and mud. Both lithofacies are overlain by an organic-rich gas-charged mud of Holocene age (typically 5 to 10 m thick) that thins and becomes more sandy above the 500-m isobath. In deeper waters, Holocene biogenic-rich mud (typically 1 to 2 m thick) overlies Late Pleistocene red mud with silt laminae in intervalley areas.

The uppermost part of the continental slope, in water depths of less than 500 to 800 m, appears smooth and undisturbed. The proglacial silts and overlying Holocene gas-charged muds in this area are truncated by a series of arcuate scarps (Fig. 3b). Both sidescan and submersible observations show large blocks of debris lying downslope from these scarps, thus indicating a probable slump origin for the scarps.

At the mouth of the Laurentian Channel is a series of steep valleys that lead from these slump scarps and coalesce near the 1,800-m isobath to form the Eastern Valley of the Laurentian Fan. Sidescan images and submersible observations suggest that these upper slope valley floors are erosional (Fig. 3c), with step-like terraces cut in stratified sediments. Blocks apparently derived from these scarps have been seen overlying a twisted cable segment near the 1,200-m isobath, indicating that the 1929 event resulted only in local erosion of the stiff mud of the valley floor in this area.

Tributary valleys west of the Eastern Valley have been eroded in older Quaternary sediments. Valley walls show a ridge and gully morphology in sidescan images (Fig. 3a). Submersible observations show that this mesotopography is highly modified by bioturbation. Comparison with the slumped areas suggests that this degree of modification requires more than 55 yr to develop, implying that there was little failure on these tributary valley walls in 1929.

Sediment failure is widespread in the soft surficial sediment of the upper St. Pierre Slope to the east of Eastern Valley, below the arcuate slump scarps. Shallow valleys lead from the slump scars (Fig. 3d) to St. Pierre Valley and Grand Banks Valley, which are larger prominent slope valleys leading to the Eastern Valley. Sidescan images and submersible observations show that

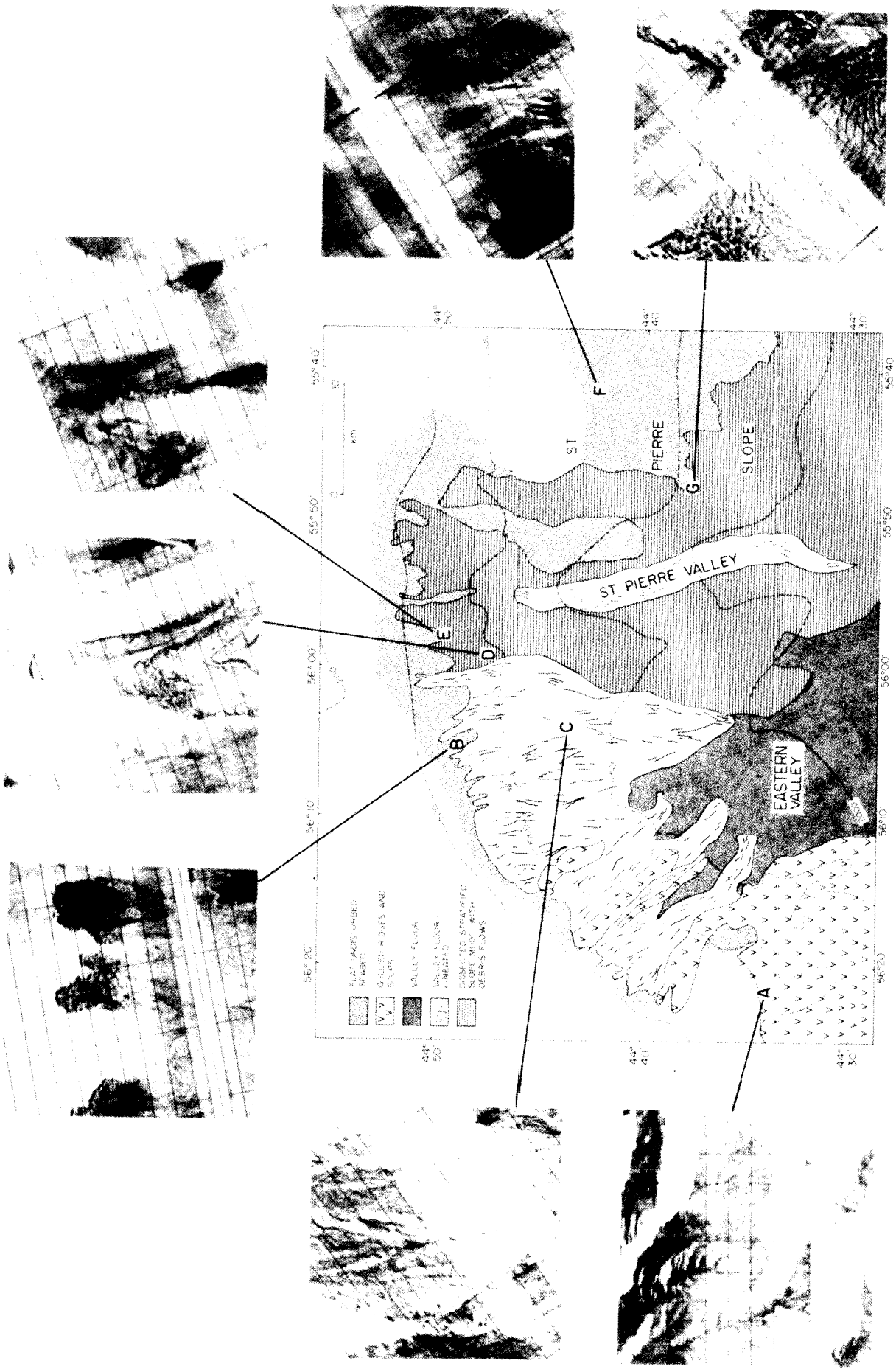

Figure 3. Morphology of the continental slope around the 1929 earthquake epicenter, illustrated by sidescan images. Each image represents 2.8 × 2.8 km^2 of sea floor: a. Ridge and gully topography. b. Arcuate slump scars on upper slope. c. Lineated erosional valley floor with pits and blocks. d. Arcuate slump scar with prominent bedding planes. e. Pockmarks (gas escape craters). f. Creased and streaked seabed. g. "Thumbprint" seabed interpreted as regressive rotational slump.

Figure 4. Photograph of Pleistocene pebbly mudstone cropping out on the floor of Eastern Valley in the epicentral region of the 1929 earthquake (1,550 m). Exhumed gravel is visible. Field of view approximately 2 by 3 m.

slumping is common on the steep valley walls. Over large areas of the slope between Eastern Valley and Grand Banks Valley, the uppermost 5 to 15 m of sediment appears to be missing on high-resolution seismic and 3.5-kHz profiles. The seabed surface commonly has a creased or streaked appearance on sidescan images (Fig. 3f), and submersible observations show a gentle undulating topography with a relief of a few meters and wavelength of tens to hundreds of meters. Where surface sediment is present, it frequently contains pockmarks, interpreted to be gas escape craters (Fig. 3e).

On the St. Pierre Slope there are large areas of seabed with prominent surface ridges a few meters high and a spacing of many tens to hundreds of meters (Fig. 3g). They occur downslope from 5 to 50-m-high scarps. Submersible observations show that these ridge crests are composed of steeply dipping stratified muds, with only limited modification by bioturbation. This "thumbprint" seabed is similar to regressive slumps on land such as the South Nation River landslip in eastern Canada (LaRochelle and others, 1970; Bentley and Smalley, 1984). Similar wrinkled topography from the Scotian Slope (Piper and others, 1985b) overlies rotational slumps, which have been sampled in several piston cores. Over much of the St. Pierre Slope, sidescan images show that the seabed is very irregular, with near-surface sediments appearing incoherent in high-resolution seismic profiles. Elsewhere, similar acoustic characteristics result from both debris flows and shallow slumps, and distinguishing between these two interpretations is not possible without more detailed local investigations.

Surface sediment failure thus appears widespread on the St. Pierre Slope. The age of this failure has not been determined directly. Seismic reflection profiles, particularly high-resolution profiles from the upper slope, show that the 30 to 100 m of sediment below the surface failures is undisturbed, suggesting that major failure occurs rarely. The distribution of surface failures seen in regional seismic reflection profiles corresponds approximately to the limit of instantaneous cable breaks in 1929. For these reasons, we consider that the surface failures that we have surveyed on the upper Laurentian Fan and St. Pierre Slope date from the 1929 earthquake, or subsequent movement of sediment made unstable during the earthquake.

SURFACE SEDIMENTS DEPOSITED BY THE 1929 EVENT

There is a distinctive suite of surface sediments in the fan valleys of the Laurentian Fan and on the Sohm Abyssal Plain that were first interpreted as the deposits of the 1929 turbidity current by Heezen and others (1954). Within the fan valleys, cores have recovered coarse sand and gravel. Some gravel at 4,700-m water depth occurs in graded, well-sorted beds as much as 5.8 m thick (Stow, 1981). These coarse sediments have been interpreted as resulting from the 1929 event because of the high velocities required to transport well-sorted gravel to these water depths. The valley floors are underlain by a discrete incoherent seismic facies, suggesting that there has been long-term accretion of coarse clastic sediments. Thus, there would have been a source of coarse sediment available on the valley floor prior to 1929 that could have been incorporated into a sufficiently competent turbidity current.

On the northern Sohm Abyssal Plain, an extensive sheet of fine sand and coarse silt exceeding 1 m thickness (Fruth, 1965) overlies pelagic sediments. A bulk sample of this pelagic material yielded a radiocarbon age of 5,130 ± 130 yr (Ericson and others, 1961), implying a late Holocene age for the thick surficial sand/silt unit. The sand sheet varies in grain size from medium to coarse sand in the valley termination zone of the Laurentian Fan to fine sand on the northern Sohm Abyssal Plain and to coarse silt near the distal limit of the sheet. The sand sheet thins from over a meter of sand to less than 10 cm of turbidite mud near its margin over a distance of less than 100 km (Piper and Aksu, 1987).

The levees of the Laurentian Fan valleys have Holocene hemipelagic sediments, overlying Pleistocene overbank turbidite silt-mud couplets (Stow and Bowen, 1980). There is no trace of a surficial turbidite mud. In the lower part of Eastern Valley, near the 4,500-m isobath, there is widespread erosion of the valley walls and an interdistributary high to about 300 m above the thalweg. These observations suggest that the 1929 turbidity current was only a few hundred meters thick and did not overtop the levees of the main fan valleys.

The volume of the deposits of the 1929 turbidity current has been estimated by Fruth (1965) as 1.4 to 1.6 × 10^{11} m^3 (i.e., about 150 km^3). At least 50 percent of the deposit is fine sand and coarse silt, and less than 10 percent is fine silt and clay.

On the Sohm Abyssal Plain, apart from the surficial sand sheet, the Holocene sequence is entirely muddy ooze. The underlying Pleistocene section is made up of thinner beds of mud, coarse silt, and sand. These are a product of the same activity that created the silt-mud couplets on the levees. Thus it appears that here has not been an event comparable to the 1929 turbidity current during at least the Holocene, which is represented by the muddy ooze.

COARSE SEDIMENTS AND BEDFORMS IN EASTERN VALLEY

Sidescan sonographs reveal a variety of flow-generated features on the Eastern Valley floor developed in sediments with a high acoustic reflectivity. We attribute these features to the passage of the 1929 turbidity current.

Eastern Valley from 1,500 m to 4,300 m is a straight, wide (more than 25 km), largely flat-floored conduit that subsequently divides into two branches (Fig. 5). The upper valley consists of a central raised floor with two marginal thalwegs cut 30 to 40 m below the main floor level (Fig. 6). In the middle reach of Eastern Valley there are two to three valley-floor channels with sections of raised floor in between. These channels appear to grow and die along the valley, but neither cut obliquely across the valley nor meander.

The Grand Banks Valley joins Eastern Valley from the

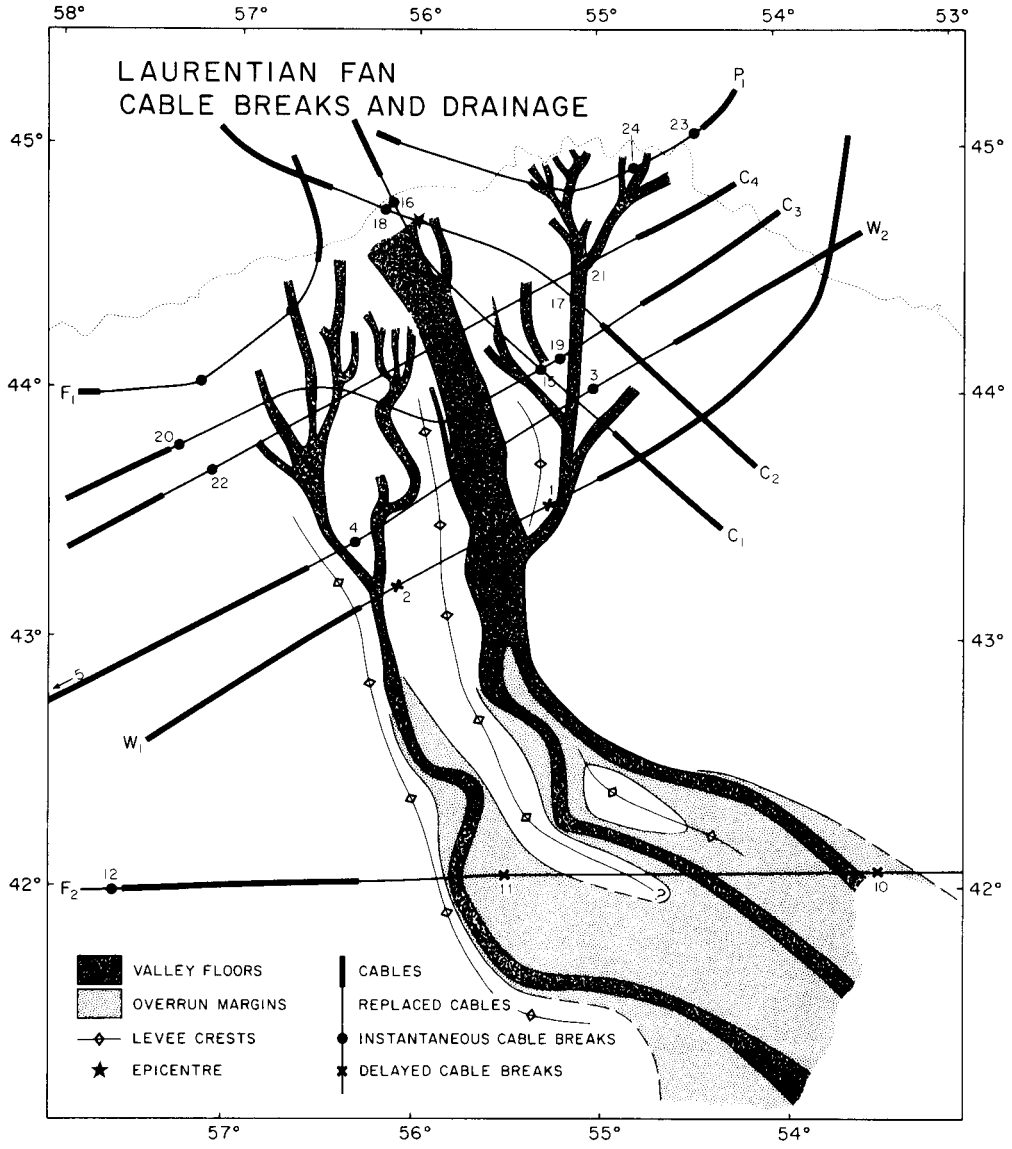

Figure 5. Diagram showing relationship of earthquake epicenter, cable locations, and cable breaks to the valley floors and margins affected by the 1929 event. Cable names and break numbers are in accordance with Doxsee (1948). Channel patterns for the upper and middle fan valleys based on Masson and others (1985).

Figure 6. Bedform succession along Eastern Valley. Nine orthorectified sidescan images are presented for the locations indicated on the valley floor. Each image represents 2.8 × 2.8 km^2 of sea floor: darker returns represent higher amplitude of acoustic backscatter. All images are oriented so that down valley is toward the bottom of the page: Images a, b, and c demonstrate the progressive evolution of the gravel waves; Images c, d, and e demonstrate the increasing importance of sand sheets; Images f and g demonstrate the periodic troughs and swells developed in places in the middle and lower valley; Image h shows the simpler morphology within the south branch of Eastern Valley; Image i shows the transverse longer-wavelength dunes developed in the valley termination zone.

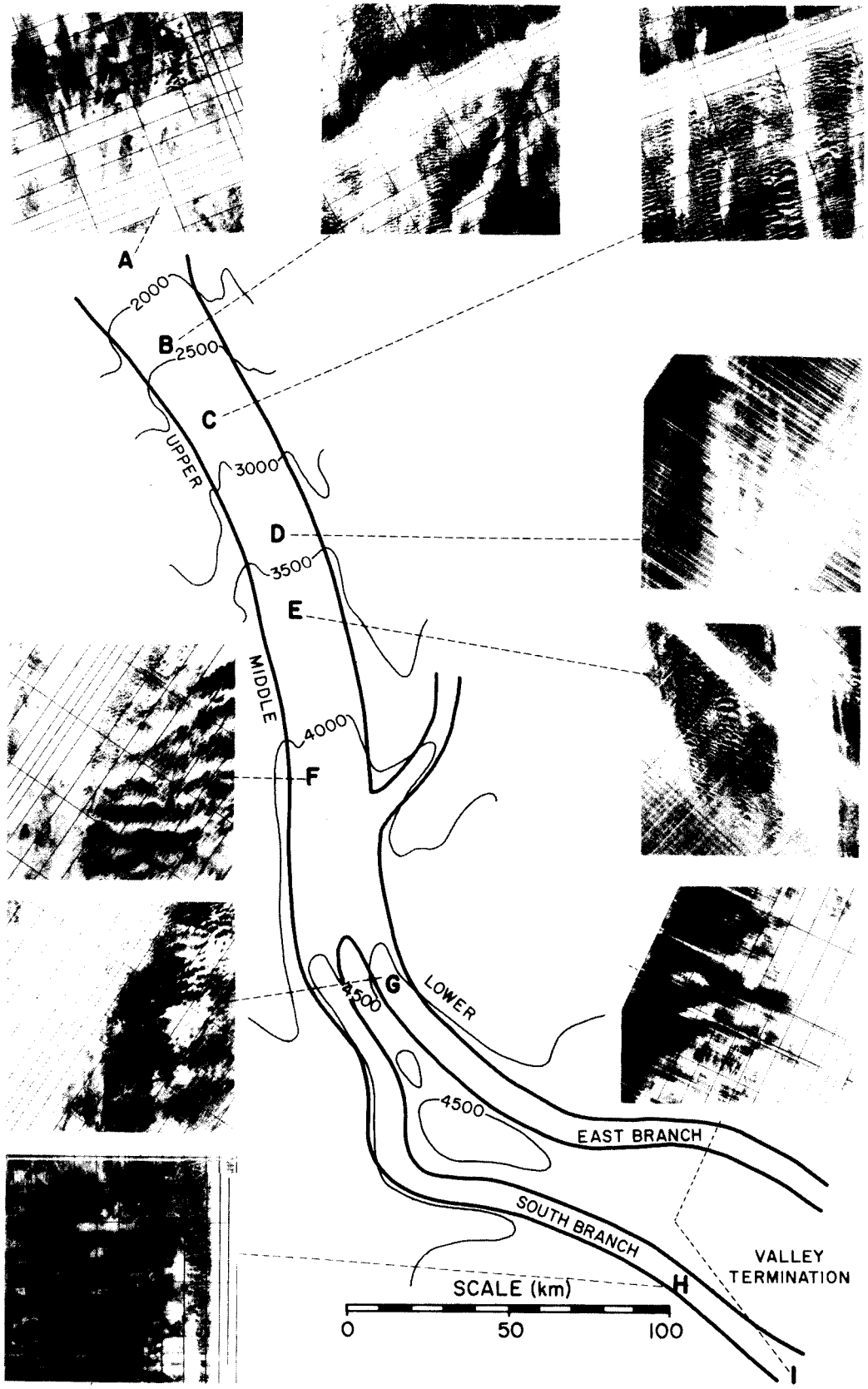

EASTERN VALLEY-BEDFORM SUCCESSION

northeast at 4,000-m water depth. The east and south branches of Eastern Valley diverge at 4,500 m. The east branch continues the trend of the main valley, curling gently to the southeast. It is the broader of the two branches. The south branch, in contrast, becomes sinuous and entrenched, and its overall morphology more closely resembles the Western Valley at this depth.

Bedforms in Eastern Valley are first observed at 1,600 m at the southern limit of the erosional lineated terrain of Piper and others (1985a). Small, poorly defined bedforms with transverse crests and a spacing of 10 to 15 m are seen in strips of higher acoustic reflectivity (darker areas in Fig. 6). By 2,300-m depth, there are well-defined higher-reflectivity regions (granule to cobble gravel) of asymmetric dunes with sinuous elongate crests transverse to inferred flow and wavelengths of 40 to 50 m that occur interspersed with smooth regions of lower-reflectivity sheets of coarse sand (Fig. 6b). At 3,000 m, the asymmetric dunes (hereafter referred to as gravel waves) are the dominant feature seen on the valley floor. They make up a wavefield broken by elongate (5 to 25 km long), thin (30 to 100 m wide) sand ribbons that are oriented downvalley (Fig. 6c). The gravel waves are best developed on elevated regions of the valley floor, whereas the sand sheets and ribbons are situated in shallow elongate depressions. The sand overlies the gravel waves and hence appears to be a late-stage deposit postdating the period of wave growth. The sand ribbons coalesce farther down the valley to form wider (600 m) composite sand sheets (Fig. 6d). By 3,500-m water depth, the smooth sand cover predominates over the gravel wavefields (Fig. 6e). From 4,000-m water depth through the east branch, to the valley termination zone, the valley is floored by sand (ribbons, sheets, and streaks) and gravel waves (wavelength 50 to 80 m), which are locally superimposed on large swells and troughs spaced 400 to 600 m apart (Fig. 6f and g). In the south branch, however, a simple axial sand belt is developed with gravel waves on either flank. Finally, in the valley termination zone, where the valley walls cease to confine larger flows, the gravel waves coexist with (Fig. 6h) and eventually are replaced by large (300-m-wavelength) transverse asymmetrical bedforms (Fig. 6i).

These features on the valley floor are built of coarse clastic sediment ranging in size from coarse sand to boulders. The gravel waves in the upper and middle valley are made up of poorly sorted cobble to granule gravel. Cores have not penetrated more than 130 cm into such coarse sediment, so that there is no information on internal structure of the gravel waves. A thin mud drape mantles the surface. Our few short cores suggest that the surface of the gravel waves is variably draped with a normally graded sand–gravel sequence. In one core, a reverse-graded gravel-sand surface layer (37 cm) overlies the normally graded sequence. From bottom photography, the surface of the waves is either smooth or appears to be a coarse lag (Fig. 7). Probing with the mechanical arm of the submersible demonstrated that the bedforms are constructed of gravel even where draped by finer sediment. The boulder lags appear on the stoss sides of the waves, whereas the lee slopes are more commonly thickly draped with sand or mud. Similar gravel bedforms have now been recognized on the floor of Nice canyon (Malinverno and others, this volume). Most sidescan surveys of deep-sea channels, however, have not found similar wave fields.

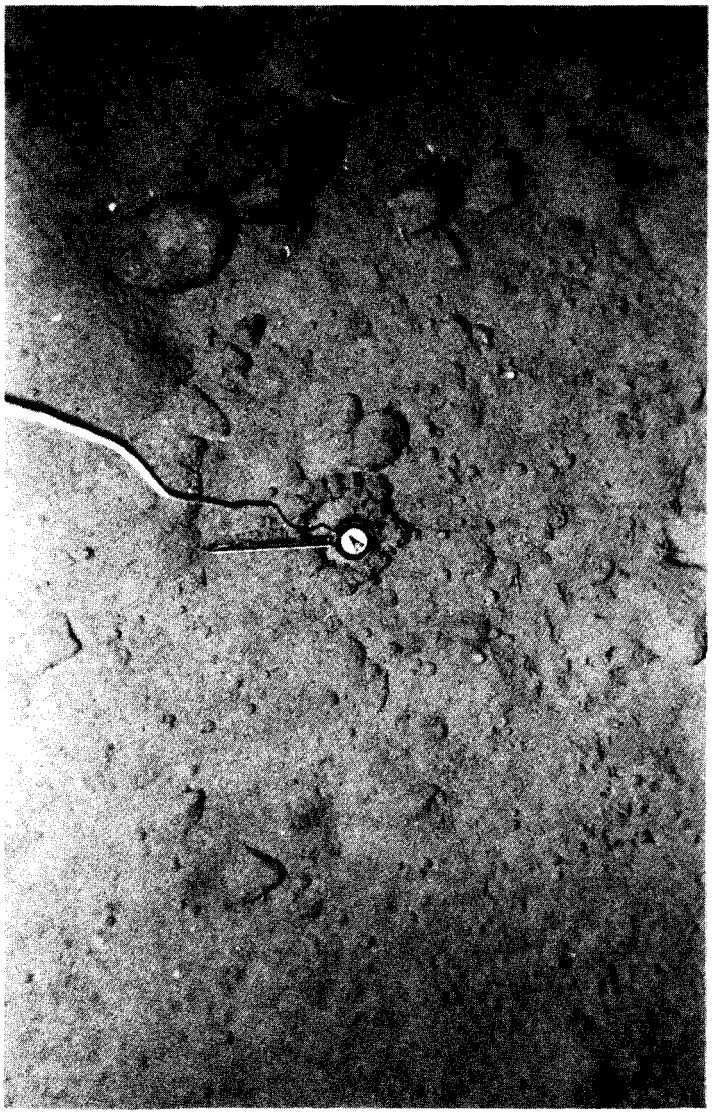

Figure 7. Photograph showing gravel pavement at 4,300 m in a gravel wave field of Eastern Valley. Cobble gravel is visible at the surface, partially covered by a thin mud drape. Field of view is 1.5 by 2.5 m.

The ribbons, in contrast, are made up of well-sorted coarse sand and granule gravel that is normally graded in the top 40 cm. In the lower Eastern Valley, cores up to 580 cm long reveal a normally graded sequence from well-sorted sand to pebble-sized (15-mm) clasts in the top 100 to 150 cm, overlying a complex alternation of variably sorted pebbly sand and gravel. Imbrication or good stratification within the coarse facies cannot be demonstrated due to disturbance during coring.

Pleistocene supply of glacial sediment to the upper slope (Stow, 1981) yielded a source of lithologically heterogeneous and poorly sorted clasts that has been incorporated into the valley floor facies. There is a downslope trend in Eastern Valley of increased sorting and decreasing grain size in the valley floor facies. The grain-size distribution is a result of varying degrees of sorting of an initially poorly-sorted, glacially derived population. The sand sheets represent a higher degree of maturity and may result from late-stage winnowing of the surface of the gravel waves.

The gravel waves imply bedload transport involving traction processes. The morphology of these gravel waves closely resembles that of the giant Scabland ripples of Washington (Bretz and others, 1956). Estimated flow depths and velocities during the formation of the Scabland ripples are 50 to 70 m and 10 to 20 m/s, with corresponding Froude numbers of 0.6 to 0.9 (Baker, 1973). By analogy with fluvial asymmetric dunes and the Scabland ripples, the gravel waves in Eastern Valley are considered to be bedforms deposited under subcritical flow conditions (Froude number <1).

COMPOSITION AND VOLUME OF FAILED SEDIMENT

The total area within which failure occurred on the continental slope in 1929 is about 20×10^9 m^2. Within this region, however, there are large areas of undisturbed surficial sediment, and it appears that only half of this area was involved in surface failure. Seismic reflection profiles on the slope off St. Pierre Bank indicate that the average thickness of missing sediment is about 5 m. If this thickness is applicable to the entire slope area, then the total volume of sediment lost would be about 100×10^9 m^3 (Piper and Aksu, 1987). On the St. Pierre Slope, slump scars cut mostly proglacial muddy sediment with an estimated 30 percent gravel, sand, and coarse silt.

The volume of gravel, sand, and coarse silt on the lower Laurentian Fan and Sohm Abyssal Plain is conservatively estimated at 175×10^9 m^3 (including sediment porosity) (Piper and Aksu, 1987). Less than 20 percent of this volume can be accounted for by the coarse sediment derived from muddy areas of the continental slope. The undisturbed nature of the entire uppermost slope means that there was no massive loss of till from the shelf break, although some distal till tongues may have failed on the slope above the Laurentian Fan. Therefore, it is necessary to postulate a large reservoir of sand in the uppermost parts of the fan valleys. This sand may have accumulated proglacially during middle Wisconsinan time when the major ice flow through the Laurentian Channel was grounded on the upper slope. During the 1929 event, a large volume of this coarse sediment was removed, perhaps by seismically induced liquefaction failure or in part by turbidity current erosion during the earthquake. Removal of 30 to 40 m of coarse sediment from the upper fan valleys would account for the observed volume of the 1929 turbidite (Piper and Aksu, 1987).

The observed volume of mud (fine silt and clay) in the 1929 turbidite is estimated as 10×10^9 m^3. This is several times less than the volume observed to be missing from the continental slope. This missing mud was probably transported southwest by deep-ocean circulation and settled out beyond the Laurentian Fan and Sohm Abyssal Plain.

ANALYSIS OF THE CABLE BREAKS

Previous work

Many authors have attempted to use the sequential cable breaks to estimate the velocity of the 1929 turbidity current. Heezen and Ewing (1952) assumed that the current advanced on a broad front and was initiated close to the epicenter. Most subsequent authors (Menard, 1964; Emery and others, 1970; Uchupi and Austin, 1979) assumed that the flow was channelized and did not make estimates based solely on the timing of the first delayed break. Differences between the estimates of various authors depend on assumptions made about the path of the current.

Significance of reported breaks

The time of a cable failure is recorded automatically by shore stations, and the position can be located in terms of the distance from the shore station (Keith, 1930). Subsequent breaks between the original break and shore station can be detected only as a drop in resistivity (Kullenberg, 1954). Thus, the time of the first break will always be known, but the second and subsequent ones may not be detected. Further breaks or damaged zones may be recognized during cable replacement.

Only two breaks were reported by de Smitt (1932) for most cables, delineating the east and west limit of breakage. The style of breaking, however, was a wide zone of parting or damage to the cables between the reported end breaks. Cables were buried but not broken on either side of the central tract where the cables had been broken and removed (Heezen and Hollister, 1971). As many as ten breaks over a distance of 140 mi went unreported for one cable. The entire section was replaced because the remaining cable was so badly damaged (Higgins, 1930).

A third break is reported for four cables. Two of these (breaks 5 and 12) occur west of the Laurentian Fan, separated from the main zone of breakage by unaffected cable (Higgins, 1930). These breaks are thus attributed to a synchronous but geographically separate event farther west on the Scotian Slope. This event must have been only minor, as cable W_1, which lies between these breaks, was unaffected.

The instantaneous breaks and slope failure

The instantaneous breaks occur on the walls of valleys and other areas of steep slopes. They may thus be attributed to slope failure resulting from the initial shock wave. The breaks delineate the limit of synchronous failure. They are not a result of passage

of turbidity current, but rather are due to dislocations of the sediment surface producing an immediate breaking stress on the cable.

The pattern of instantaneous cable breaks indicates that an area of roughly 100 km in diameter around the epicenter experienced simultaneous local mass wasting. Thus we cannot identify a point source for the turbidity current against which the first delayed breaks (numbers 1 and 2) can be referenced. Estimates of flow velocity based on travel times from the epicenter to the first delayed breaks (Heezen and Ewing, 1952) are thus unreliable.

Delayed breaks and the turbidity current

Subsequent breaks may be attributed to downslope passage of mobile sediment in a turbidity current. Delayed breaks 1 and 2 are positioned at the confluence of the Western and Central Valleys and slightly up the Grand Banks Valley from the zone of confluence with the Eastern Valley (Fig. 5). Thus the passage of the turbidity current head down the Western or Central and Grand Banks Valleys was apparently faster than down the Eastern Valley (which lies in the middle of the broken cable segments).

The next delayed break, number 11, is situated on the margin of the Western Valley, delineating the western limit of cable damage. The time of the subsequent break delineating the eastern limit (number 10 in the east branch of Eastern Valley) is unknown. This again suggests a faster passage down the Western Valley than the Eastern Valley (the Grand Banks and Central Valleys are no longer discrete features at this latitude). A minimum velocity of 19 m/s can be calculated for the head of the turbidity current down the Western Valley between breaks 2 and 11 (measuring the straight-line distance between the two breaks). If the path of the current followed the axis of Western Valley, then a velocity of 20 m/s is obtained. These estimates are almost identical to those of Menard (1964) and Uchupi and Austin (1979), and represent the maximum demonstrable velocity for the turbidity current.

FLOW CONDITIONS IN THE TURBIDITY CURRENT

The character of turbidity current flow in Eastern Valley can be determined in some detail, because we know the floor slope, the valley cross section, and an upper limit on the velocity from cable breaks in the Western Valley. We also have limited information on the sediment transported, and a variety of observations to constrain the flow thickness. All of these parameters vary down valley. We have focused, therefore, on the middle reach of Eastern Valley at 43°N in about 4,400-m water depth, as it was sufficiently far away from the source region for the flow to be approaching a steady-state condition, yet was still constrained within the valley. Furthermore, this location is below the confluence with the Grand Banks Valley, so that its contribution is included. At this location, the slope is 5×10^{-3}.

Previous estimates in other deposits of current velocity from valley-floor facies (e.g., Komar, 1969; Walker, 1975; Winn and Dott, 1977, 1979) have used the estimated threshold velocity for bedload transport of the largest observed clast and the velocity required to transport an inferred suspended load.

In Eastern Valley, the observations on maximum clast size are limited to sparse bottom-camera coverage of the top of the clastic sequence. Submersible observations are available at 2,000-m water depth, where 2-m boulders have been observed on the valley floor. In the middle valley, around 4,000 m, a maximum size of 50 cm has been observed in bottom photographs; and in the lower valley, there do not appear to be surface boulders, as the floor is covered by a thick, surface, accretionary, graded layer of gravel to mud. In the upper valley, it is not known whether the boulders have been merely exhumed in place from outcrop (as has been observed from submersible), or whether they have been truly transported.

The thick, graded gravel in the lower valley (Stow, 1981), with a median grain size of about 15 mm at the bottom of the core, is interpreted as a suspension load deposit. Using the suspension criteria of Bagnold (1966) and Bridge (1981), this corresponds to flow velocities of the order of 13 to 16 m/s.

Estimates of bedload and suspended-load threshold criteria for such coarse clastics, however, are poorly constrained by empirical data. Bedload thresholds are hard to define for natural poorly sorted deposits and have been demonstrated to also be a function of hydraulic radius (Carling, 1983) and sorting (relative protrusion, Hammond and others, 1984), as well as the grain size, shape, and density. Empirical calibration of suspension criteria has not been made for coarse clasts under conditions of high sediment concentration. For these reasons, we do not place much reliance on estimates of flow velocity from grain size.

Flow thickness can be physically constrained in the middle reach of Eastern Valley to between 270 and 420 m, on the basis of erosional lineations and the surface distribution of coarse sediment as interpreted from sidescan sonographs and 12-kHz profiles. We can also use the presence of the gravel waves to constrain the flow thickness by two methods. First, the gravel waves are interpreted as subcritical bedforms, the internal Froude number of the flow must have been less than unity (at least for the period of bedform growth). Second, Baker (1973, Fig. 51) was able to demonstrate an empirical relationship between the depth (D)–slope (S) product and the ripple chords (wavelengths) of the giant Scabland ripples:

$$\text{chord} = 263.7 \cdot (D \cdot S)^{0.66}$$

If allowance is made for the smaller density contrast, the following empirical relationship may be used for the gravel waves:

$$\text{chord} = 263.7 \cdot \left[\left(\frac{\rho_t - \rho}{\rho_t}\right) \cdot D \cdot S\right]^{0.66} \quad (1)$$

To use these relationships, an estimate of flow density is necessary. Kuenen (1952) suggested a density of 1,600 kg/m^3 for

the 1929 turbidity current. More recent work, however, suggests that this density is far too great for natural turbidity currents. Bagnold (1954) suggested that grain-to-grain interaction dominates when the volume concentration of the sediment exceeds 9 percent (1,173 kg/m^3 for a grain density of 2,650 kg/m^3). Densities estimated for sandy turbidity currents range from 1 to 7 percent (Bowen and others, 1984, Fig. 12), in contrast with values as low as 0.1 percent for muddy turbidity currents (Stow and Bowen, 1980). The 1929 current did mobilize cobbles and boulders, but they were probably moved as bedload. In the lower valley, a mean grain size of 15 mm is found at the base of graded cores, implying deposition from suspended load. Thus, this turbidity current was exceptionally coarse, and for our calculations we have taken a relatively high value of 6 percent (1,124 kg/m^3) as an estimate for the density.

Using the first method, we estimate that at the upper limit of velocity (19 m/s), the flow depth must have exceeded 397 m (and would be 186 m for 13 m/s). Using the second method, for observed chords of 50 to 80 m, the calculated flow thicknesses are 186 to 379 m. This flow thickness would correspond to the body of the turbidity current during the period of bedform growth.

Thus, a variety of methods all indicate maximum flow thicknesses of the order of 300 to 400 m. In the analysis below, we therefore examine two cases: one for a thickness of 300 m, the other 400 m. We apply standard equations of flow (Komar, 1969) to examine the flow conditions of the 1929 turbidity current in the middle reach of Eastern Valley.

Chezy-type equation for steady-state flow can be derived from the Bagnold equation (Komar, 1969; Bagnold, 1962):

$$u = \left[\frac{(\rho_t - \rho)}{(\rho_t)} \cdot \frac{g \cdot h_b \cdot S}{(1 + \alpha)\, C_f} \right]^{1/2} \quad (2)$$

and estimates of head velocity can be made using Middleton's (1966) equation:

$$v = 0.75 \left[\frac{(\rho_t - \rho)}{(\rho_t)} \cdot g \cdot h_h \right]^{1/2} \quad (3)$$

where u = body velocity, v = head velocity, ρ_t = current density, ρ = seawater density (1027 kg/m^{-3}), h_b = body thickness, h_h = head thickness, S = slope (5×10^{-3}), α = ratio of interfacial shear to bed shear (0.43), and C_f = drag coefficient.

In previous numerical modeling of flows in turbidite channels, the appropriate values for bed roughness have been a matter of controversy (Komar, 1975; Hand, 1974). This was in part because the contribution of isolated roughness elements—like megaflutes (Lonsdale and Hollister, 1979) and other erosional features (McGregor and others, 1982)—to overall channel drag was hard to quantify. The gravel wave field, however, covers almost the whole of the upper valley floor and rarely less than half of the floor in the middle and lower valley.

If we take the gravel waves as bed roughness elements of the order of 5 m amplitude, using the Von Karman–Prandtl equation for a rough bed, the drag coefficient is between 4.5 and 4.1×10^{-3} for flow thicknesses of 300 to 400 m. We, therefore, use a value of 4.3×10^{-3}, which is higher than has been used in most other studies in the deep sea (e.g., 3.5×10^{-3}, for the Maury Channel, Lonsdale and others, 1981), reflecting the additional presence of the gravel waves.

The flow velocity of 19 m/s obtained from the Western Valley is taken as an upper limit for the head velocity. Using estimates of flow thickness of 300 and 400 m (which may be either a body or a head thickness) in equations 2 and 3, we obtain the following velocity estimates: for head thicknesses of 300 and 400 m, head velocities of 12.0 and 13.8 m/s; for body thicknesses of 300 and 400 m, body velocities of 14.4 and 16.6 m/s; a corresponding subcritical Froude number of 0.88.

Estimates of discharge and duration of the flow depend on body velocity. The above estimates of body velocity give discharges between 1.1 and 1.7×10^8 m^3/s. If we assume that two-thirds of the volume of sediment in the turbidite (with 40 percent porosity) on the Sohm Abyssal Plain passed through the middle reach of Eastern Valley, a flow concentration of 6 percent by volume implies the minimum duration of turbidity current flow was 3 to 2 hr. The actual flow duration probably exceeded this estimate, however, because both flow velocity and concentration would have decreased in the later stages of the flow.

DISCUSSION

Recurrence interval

Earthquakes of magnitude sufficient to cause widespread sediment failure occur somewhere on the eastern Canadian continental margin every few hundred years (Basham and Adams, 1983). For example, there were large earthquakes in southern Baffin Bay in 1931 and off central Labrador in the nineteenth century. Piper and others (1985b) recognized widespread slumping on the central Scotian Slope caused by a large earthquake about 12,000 yr ago. There is, however, no evidence of a very large earthquake affecting the upper Laurentian Fan for many thousands of years before the 1929 event (Piper and Normark, 1982a).

No other thick, widespread, sandy turbidite is known in the upper 10 m of sediment on the eastern Canadian continental margin. This implies that the 1929 turbidite was an unusual event resulting from the fortuitous occurrence of a large earthquake near a large glacial depocenter on the steep upper continental slope. Furthermore, the peculiar topography of the Laurentian Fan, with a large number of upper slope valleys focused into two main fan valleys with very high relict levees, allowed a confined high-density flow to maintain itself across the slope and rise. Thus, a large volume of sediment was transported to the deep sea, rather than being redeposited on the slope and upper rise.

Fan and abyssal plain growth

The 1929 event has been taken as a type example of a dense, sandy turbidity current. Its thick, sandy deposit, with distinctive

proximal to distal changes in grain size and bedforms, would have a high preservation potential in the ancient record, but for its location on oceanic crust. In contrast, lower-density, thicker, muddy turbidity currents are almost certainly a more important mechanism for the long-term accretion of the fan. Sandy turbidity currents of the magnitude of the 1929 event are too infrequent to make a major volumetric contribution. Such coarse units might be thought important to the growth of abyssal plains, because they form mappable marker horizons. Volumetrically, however, they may be overemphasized because they are more easily correlatable than silt or mud units.

During Wisconsinan time, bankfull turbidity currents capable of moving silt and clay appear to be the more common type of event on the Laurentian Fan (Stow and Bowen, 1980). Triggering of these events was much more frequent; they were a response to rapid deposition on the upper slope as a result of glacially controlled outwash and iceberg melting. Under these conditions, failure may have been induced by small earthquakes, large dropstones, storm waves, or even whale impacts (Ryan, 1982).

Although turbidites like the 1929 deposit are volumetrically of minor significance on the fan, such large turbidity currents are of great importance in controlling its growth pattern. The 1929 event flushed out the fan valleys: without such a process, the valleys would tend to aggrade in the manner seen on many large passive-margin fans (such as the Bengal Fan; Emmel and Curray, 1984), resulting in channel migration by avulsion.

The erosive power of the 1929 turbidity current was related to its large load of sand and gravel. In most passive-margin deep-sea fans, gravel and coarse sand are not available in the source sediment for turbidity currents: such coarse clastics are trapped in terrestrial deposits in the hinterland. The coarse sediment supply to the 1929 turbidity current is the result of a glacial source. Fan systems supplied by fan deltas in orogenically active areas also have a significant source of coarse sediments, so that it is in these environments that ancient analogues of the 1929 event might be sought.

The volume of the 1929 turbidite is similar to that of "seismoturbidites," which Mutti and others (1984) describe as occurring intercalated within normal flysch sequences. The 1929 turbidite differs from many typical carbonate-rich seismoturbidites in lacking a basal breccia in most areas. Furthermore, the 1929 turbidites do show systematic proximal to distal changes in grain size and in sedimentary structures, as far as they can be inferred from surficial bedforms. The very well developed preexisting valley system on the Laurentian Fan may have played an important role in focusing and confining the turbidity current, compared with many seismoturbidites that are inferred to have traveled more as sheet flows across slopes with lesser bathymetric relief. The cable breaks provide evidence for sediment failures over a wide source area, as is inferred for other seismoturbidites. The sediment budget calculations, however, indicate that most of the sediment in the 1929 turbidite was derived from reservoirs of coarse sediment in the heads of the fan valleys, rather than from regional failure of continental slope sediments. The widely observed down-fan decrease in the frequency of turbidity currents (Piper and Normark, 1983, Figs. 8 and 9) suggests that fan valleys may be an important reservoir of coarse sediment to many fans. Flushing of fan valleys may thus provide a mechanism for supplying clastic sediment to extremely large turbidites.

CONCLUSIONS

The 1929 sediment failure and resulting turbidity current was an impressive convulsive event. Transatlantic communications were disrupted for six months. There was sediment failure over an area of 20,000 km^2 on the continental slope. As much as 200 km^3 of sediment was transported in the turbidity current, flowing with thicknesses of a few hundred meters and velocities up to 19 m/s. Graded beds of gravel were deposited more than 300 km from the shelf break, and a bed of sand more than 1 m thick was deposited over an area of 150,000 km^2 on the Sohm Abyssal Plain. Where the flow was confined within the fan valleys, it molded the coarse seabed sediments into a series of bedforms. Gravel wave fields in the upper valley became increasingly masked by sand sheets and ribbons downvalley, and long-wavelength, symmetrical, sandy bedforms predominate in the lower valley.

Although the 1929 turbidite is not of major volumetric importance on the fan, the behavior of the 1929 turbidity current was important for the overall growth pattern of the fan. Flushing of sediment from the upper valley system, such as occurred in the 1929 event, prevents aggradation of the valley system, a process which occurs in many large passive-margin deep-sea fans and which eventually leads to channel avulsion.

The 1929 event was an unusual occurrence, resulting from the fortuitous coincidence of a large earthquake at the site of a large accumulation of coarse Upper Pleistocene sediment on the steep continental slope. Many of the distinctive features of the turbidite on the Laurentian Fan are the result of the large amount of gravel available to the turbidity current. Similar turbidites in the ancient geologic record occur not only in glaciated terrains, but also in orogenic belts where coarse sediment is delivered to the coastline by fan deltas.

REFERENCES CITED

Bagnold, R. A., 1954, Experiments on gravity free dispersion of large solid spheres in a Newtonian fluid under stress: Proceedings of the Royal Society of London, A, v. 225, p. 49–63.

—— , 1962, Auto suspension of transported sediments; Turbidity currents: Proceedings of the Royal Society of London, A, v. 265, p. 315–319.

—— , 1966, An approach to the sediment transport problem from general physics: U.S. Geological Survey Professional Paper 422–I, 37 p.

Baker, V. R., 1973, Paleohydrology and sedimentology of Lake Missoula flooding in eastern Washington: Geological Society of America Special Paper 144, 73 p.

Basham, P., and Adams, J., 1983, Earthquakes on the continental margin of eastern Canada; Need future large events be confined to the locations of large historical events?, *in* The 1886 Charleston earthquake and its implication for today: U.S. Geological Survey Open-File Report 83–842, p. 456–467.

Bentley, S. P., and Smalley, I. J., 1984, Landslips in sensitive clays, *in* Brunsden, D., and Prior, D. B., eds., Slope instability: New York, J. Wiley, p. 457–490.

Bowen, A. J., Normark, W. R., and Piper, D.J.W., 1984, Modelling of turbidity currents on Navy submarine fan, California continental borderland: Sedimentology, v. 31, p. 169–185.

Bretz, J. H., Smith, H.T.U., and Neff, G. E., 1956, Channeled Scablands of Washington; New data and interpretations: Geological Society of America Bulletin, v. 67, p. 957–1049.

Bridge, J. S., 1981, Hydraulic interpretation of grain size distributions using a physical model for bedload transport: Journal of Sedimentary Petrology, v. 51, p. 1109–1124.

Carling, P. A., 1983, Threshold of coarse sediment transport in broad and narrow natural streams: Earth Surface Processes and Landforms, v. 8, p. 1–18.

de Smitt, V. P., 1932, Earthquakes in the North Atlantic as related to submarine cables: EOS Transactions of the EOS American Geophysical Union, p. 103–109.

Dewey, J. W., and Gordon, D. W., 1984, Map showing recomputed hypocenters of earthquakes in the eastern and central United States and adjacent Canada: U.S. Geological Survey Miscellaneous Field Studies Map MF–1699, scale 1:2,500,000.

Doxsee, W. W., 1948, The Grand Banks earthquake of November 18, 1929: Ottawa, Publications of the Dominion Observatory, v. 7, no. 7, p. 323–335.

Emery, K. O., Uchupi, E., Phillips, J. D., Bowin, C. O., Bunce, E. T., and Knott, S. T., 1970, Continental rise off eastern North America: American Association of Petroleum Geologists Bulletin, v. 54, p. 44–108.

Emmel, F. J., and Curray, J. R., 1984, The Bengal submarine fan, northeastern Indian Ocean: Geo-Marine Letters, v. 3, p. 119–124.

Ericson, D. B., Ewing, M., Wollin, G., and Heezen, B. C., 1961, Atlantic deep-sea sediment cores: Geological Society of America Bulletin, v. 72, p. 193–286.

Fruth, L. S., 1965, The 1929 Grand Banks turbidite and the sediments of the Sohm Abyssal Plain [M.Sc. thesis]: New York, Columbia University, 258 p.

Hammond, F.D.C., Heathershaw, A. D., and Langhorne, D. N., 1984, A comparison between Shields threshold criterion and the movement of loosely packed gravel in a tidal channel: Sedimentology, v. 31, p. 51–62.

Hand, B. M., 1974, Supercritical flow in density currents: Journal of Sedimentary Petrology, v. 44, p. 637–648.

Haworth, R. T., and Keen, C. E., 1979, The Canadian Atlantic margin; A passive margin encompassing an active past: Tectonophysics, v. 59, p. 83.

Heezen, B. C., and Ewing, W. M., 1952, Turbidity currents and submarine slumps, and the 1929 Grand Banks earthquake: American Journal of Science, v. 250, p. 849–873.

Heezen, B. C., and Hollister, C. D., 1971, The face of the deep: New York, Oxford University Press, 659 p.

Heezen, B. C., Ericson, D. B., and Ewing, W. M., 1954, Further evidence for a turbidity current following the 1929 Grand Banks earthquake: Deep-Sea Research, v. 1, p. 193–202.

Higgins, 1930, in discussion following paper by Hodgson and Doxsee: Eastern Section of the Seismological Society of America, Proceedings of the 1930 Meeting, Washington, D.C., p. 79–81.

Hughes Clarke, J. E., 1986, Surficial morphology of Eastern Valley, Laurentian Fan: Geological Survey of Canada Open File 1425, 22 p.

Keith, A., 1930, The Grand Banks earthquake: Eastern Section of the Seismological Society of America, Supplement to the Proceedings of the 1930 Meeting, Washington, D.C., p. 1–9.

King, L. H., and MacLean, B., 1970, Origin of the outer part of the Laurentian Channel: Canadian Journal of Earth Sciences, v. 7, p. 1470–1484.

Komar, P. D., 1969, The channelised flow of turbidity currents with application to Monterey Deep-sea Fan Channel: Journal of Geophysical Research, v. 78, no. 18, p. 4544–4558.

—— , 1975, Supercritical flow in density current; A discussion: Journal of Sedimentary Petrology, v. 45, p. 747–749.

Kuenen, P. H., 1952, Estimated size of the Grand Banks turbidity current: American Journal of Science, v. 250, p. 874–884.

Kullenberg, B., 1954, Remarks on the Grand Banks turbidity current: Deep-Sea Research, v. 1, p. 203–210.

LaRochelle, P., Changnon, J. Y., and Lefebvre, G., 1970, Regional geology and landslides in marine clay deposits of eastern Canada: Canadian Geotechnical Journal, v. 7, p. 145–156.

Lonsdale, P., and Hollister, C. D., 1979, Cut-offs at an abyssal meander south of Iceland: Geology, v. 7, p. 597–601.

Lonsdale, P., Hollister, C. D., and Mayer, L., 1981, Erosion and deposition in interplain channels of the Maury Channel system, northeast Atlantic: Oceanologica Acta, v. 4, no. 2, p. 185–201.

Masson, D. G., Gardner, J. V., Parson, L. M., and Field, M. E., 1985, Morphology of upper Laurentian Fan using GLORIA long-range sidescan sonar: American Association of Petroleum Geologists Bulletin, v. 69, p. 950–959.

McGregor, B. Stubblefield, W. L., Ryan, W.B.F., and Twitchell, D. C., 1982, Wilmington submarine canyon; A marine fluvial-like system: Geology, v. 10, p. 27–30.

Meagher, L., 1984, Interpretation of Quaternary and Upper Neogene seismic stratigraphy on the continental slope off St. Pierre Bank: Geological Survey of Canada Open File 1077, 10 p.

Menard, H. W., 1964, Marine geology of the Pacific: New York, McGraw Hill Book Co., 271 p.

Middleton, G. V., 1966, Experiments on density and turbidity currents; I. Motion of the head: Canadian Journal of Earth Sciences, v. 3, p. 523–546.

Mutti, E., Ricci Lucchi, F., Seguret, M., and Zanzucchi, G., 1984, Seismoturbidites; A new group of resedimented deposits: Marine Geology, v. 55, p. 103–116.

Normark, W. R., Piper, D.J.W., and Stow, D.A.V., 1983, Quaternary development of channels, levees, and lobes on middle Laurentian Fan: American Association of Petroleum Geologists Bulletin, v. 67, p. 1400–1409.

Piper, D.J.W., and Aksu, A. E., 1987, The source and origin of the 1929 Grand Banks turbidity current inferred from sediment budgets: Geo-Marine Letters, v. 7, p. 177–182.

Piper, D.J.W., and Normark, W. R., 1982a, Effect of the 1929 Grand Banks earthquake on the continental slope off eastern Canada, *in* Current research, Part B: Geological Survey of Canada Paper 82–1B, p. 147–151.

—— , 1982b, Acoustic interpretation of Quaternary sedimentation and erosion on the channeled upper Laurentian Fan, Atlantic margin of Canada: Canadian Journal of Earth Sciences, v. 19, p. 1974–1984.

—— , 1983, Turbidite depositional patterns and flow characteristics, Navy submarine fan, California borderland: Sedimentology, v. 30, p. 681–694.

Piper, D.J.W., Stow, D.A.V., and Normark, W. R., 1984a, The Laurentian Fan; Sohm Abyssal Plain: Geo-Marine Letters, v. 3, p. 141–146.

Piper, D.J.W., Sparkes, R., Mosher, D. C., Shor, A. N., and Farre, J. A., 1984b, Seabed instability near the epicentre of the 1929 Grand Banks earthquake: Geological Survey of Canada Open File 1131, 29 p.

Piper, D.J.W., Shor, A. N., Farre, J. A., O'Connell, S., and Jacobi, R., 1985a, Sediment slides and turbidity currents on the Laurentian Fan; Side-scan sonar investigations near the epicentre of the 1929 Grand Banks earthquake: Geology, v. 13, p. 538–541.

Piper, D.J.W., Farre, J. A., and Shor, A. N., 1985b, Scotian Slope: Geological Society of America Bulletin, v. 96, p. 1508–1517.

Ryan, W.B.F., 1982, Interrelationship between oceanographic events and mass wasting of the seafloor, *in* Saxov, S., and Nieuwenhuis, J. K., eds., Marine slides and other mass movements: NATO Conference Series IV, Marine Science, v. 6, p. 263.

Stow, D.A.V., 1984, Laurentian Fan; Morphology, sediments processes, and growth pattern: American Association of Petroleum Geologists Bulletin, v. 65, p. 375–393.

Stow, D.A.V., and Bowen, A. J., 1980, A physical model for the transport and sorting of fine-grained sediment by turbidity currents: Sedimentology, v. 27, p. 31–46.

Uchupi, E., and Austin, J. A., Jr., 1979, The stratigraphy and structure of the Laurentian Cone region: Canadian Journal of Earth Sciences, v. 16, p. 1726–1752.

Walker, R. G., 1975, Generalized facies models for resedimented conglomerates of turbidite association: Geological Society of America Bulletin, v. 86, p. 737–748.

Winn, R. D., Jr., and Dott, R. H., Jr., 1977, Large scale traction produced structures in deep-water fan-channel conglomerates in southern Chile: Geology, v. 5, p. 41–44.

—— , 1979, Deep-water fan-channel conglomerates of Late Cretaceous age, southern Chile: Sedimentology, v. 26, p. 203–208.

Revised Manuscript Received November 1, 1986
Manuscript Accepted by the Society April 4, 1988